Supporting information for "A detailed mechanistic study of bulk MADIX of styrene and its chain extension"

Dries J.G. Devlaminck[a], Paul H.M. Van Steenberge,[a] Lies De Keer,[a] Marie-Françoise Reyniers,[a] Dagmar R. D'hooge*[a,b]

[a]Laboratory for Chemical Technology, Ghent University, Technologiepark 914, B-9052 Ghent, Belgium.

[b]Centre for Textile Science and Engineering, Ghent University, Technologiepark 907, B-9052 Ghent, Belgium.

Corresponding author: dagmar.dhooge@ugent.be

Table of contents

S1. Overview of the experimental conditions: homopolymerization

Table S1: Overview of the initial conditions used in the experimental study of homopolymerization MADIX of styrene at 70°C, selecting OEXEP as initial RAFT agent and AIBN as conventional initiator; 4 m% *n*-decane was added as internal standard for GC analysis; $V_{Sty,0}$=35 mL.

Entry	$[Sty]_0$	$[Sty]_0/[OEXEP]_0$	$[OEXEP]_0/[AIBN]_0$	$[Sty]_0/[OEXEP]_0/[AIBN]_0$
1	7.56	50	30	50/1/0.033
2	7.55	50	10	50/1/0.1
3	7.53	50	5	50/1/0.2
4	7.51	40	50	40/1/0.02
5	7.68	100	20	100/1/0.05
6	7.76	200	10	200/1/0.1
7	7.67	100	10	100/1/0.1

S2. Synthesis procedure of (O-ethyl xanthate)-2-ethyl propionate (OEXEP), the initial RAFT agent (R_0X) used in this work

OEXEP was synthesized according to the literature procedure.[1] Ethyl 2-bromopropionate (50.3 g, 0.278 mol) was dissolved in 500 mL ethanol and mixed with potassium O-ethyl dithiocarbonate (50.7 g, 0.316 mol) under argon atmosphere. The mixture was stirred for 6 hours in the absence of light at 0°C. Afterwards 500 mL water was added and the obtained OEXEP was extracted by a 1:2 (v:v) mixture of diethyl ether and pentane. The solvent and residual ethyl 2-bromopropionate were removed by evaporation under vacuum. Upon analysis (see Section S3 of the Supporting Information) a product molar purity of 97±1% was obtained.

S3. Determination of purity of (O-ethyl xanthate)-2- ethyl propionate (OEXEP)

The purity of OEXEP, synthesized according to the procedure mentioned in the Section S2, has been determined by means of ^{1}H NMR analysis (Figure S1 ,left) of the obtained product and following equation:

$$molar\ purity = \frac{\int D}{\int D + \int H} = \frac{3.00}{3.00 + 0.08} = 0.974 \tag{S1}$$

Ethyl 2-bromopropionate can be identified as main impurity and no other significant impurities or side products could be detected, as confirmed by GC analysis (Figure S1 ,right).

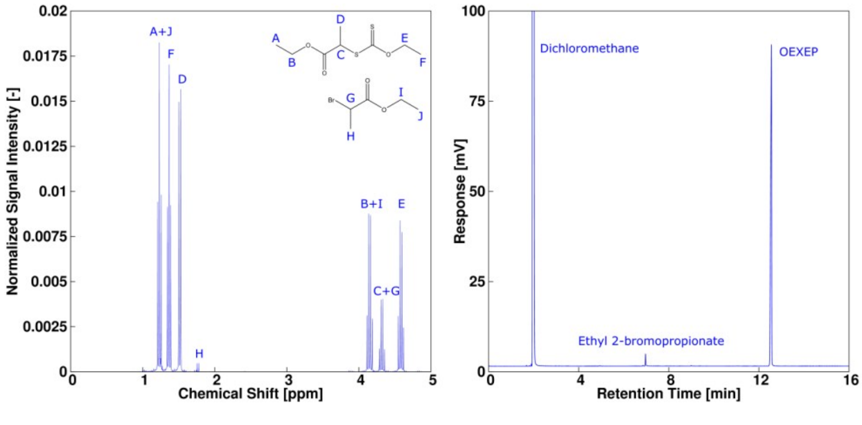

Figure S1: ^{1}H NMR (left) and GC (right) analysis of the synthesized OEXEP used as initial RAFT agent in the present work

S4. Overview of the experimental conditions: chain extension with styrene

Table S2: Overview of the initial conditions used in the experimental study of MADIX chain extension with styrene at 70°C; the initial polystyrene was obtained by purifying the product of Entry 3 in Table S1 after 8h of reaction time; AIBN was used as conventional initiator; 4 mt% *n*-decane was added as internal standard for GC analysis; with $[RX]_0$ the concentration of dormant polystyrene as determined by Equation 7 of the main text.

Entry	$[Sty]_0$	$[MSty]_0/[RX]_0$	$[RX]_0/[AIBN]_0$	$[Sty]_0/[RX]_0/[AIBN]_0$
1	6.07	175	20	175/1/0.05
2	4.93	85	25	85/1/0.04
3	5.06	95	100	95/1/0.01

S5. Justification of the Equation 7 of the main text

The number average chain length x_n can be written as the ratio of the sum of the first moment of the dead, living and dormant species to the zero moment of these species:

$$x_n = \frac{\sum_{i=1}^{\infty} i([P_i] + [R_i] + [R_iX])}{\sum_{i=1}^{\infty} ([P_i] + [R_i] + [R_iX])} \quad \text{(S2)}$$

As $[A] = \frac{n_A}{V}$ with $[A]$ the concentration of A, n_A the molar amount of A and V the volume:

$$x_n = \frac{\sum_{i=1}^{\infty} i\frac{1}{V}\left(n_{P_i} + n_{R_iX} + n_{R_i}\right)}{\sum_{i=1}^{\infty} \frac{1}{V}\left(n_{P_i} + n_{R_iX} + n_{R_i}\right)} \quad \text{(S3)}$$

Multiplying each side with the molar amount of all RiX species:

$$x_n \sum_{i=1}^{\infty}\left(n_{R_iX}\right) = \frac{\sum_{i=1}^{\infty} i\left(n_{P_i} + n_{R_iX} + n_{R_i}\right)}{\sum_{i=1}^{\infty}\left(n_{P_i} + n_{R_iX} + n_{R_i}\right)} \sum_{i=1}^{\infty}\left(n_{R_iX}\right) \quad \text{(S4)}$$

The amount of dormant chains can be related to the end-group functionality (EGF):

$$x_n \sum_{i=1}^{\infty}\left(n_{R_iX}\right) = \sum_{i=1}^{\infty} i\left(n_{P_i} + n_{R_iX} + n_{R_i}\right) EGF \quad \text{(S5)}$$

Rearranging and multiplying both the numerator and denominator of the right hand side with the monomer molar mass M_{sty} results in the equation of the molar amount of R_iX as mentioned in the main text (Equation 7).

$$\sum_{i=1}^{\infty}\left(n_{R_iX}\right)=\frac{M_{Sty}\sum_{i=1}^{\infty} i\left(n_{P_i}+n_{R_iX}+n_{R_i}\right)}{M_{Sty}\,x_n}EGF \tag{S6}$$

$$n_{R_iX}=\frac{m_{PS}}{M_n}EGF \tag{S7}$$

S6. Confirmation of accuracy of conversion determination by gas chromatography

Monomer and RAFT agent conversion (X_m and X_{R0X}) were determined by means of gas chromatography (GC), as explained in the main text. The accuracy of the technique can be verified by ^{1}H nuclear magnetic resonance (NMR). As shown in Figure S2, the conversion values obtained by both techniques are in excellent agreement (entry 7 in Table S1).

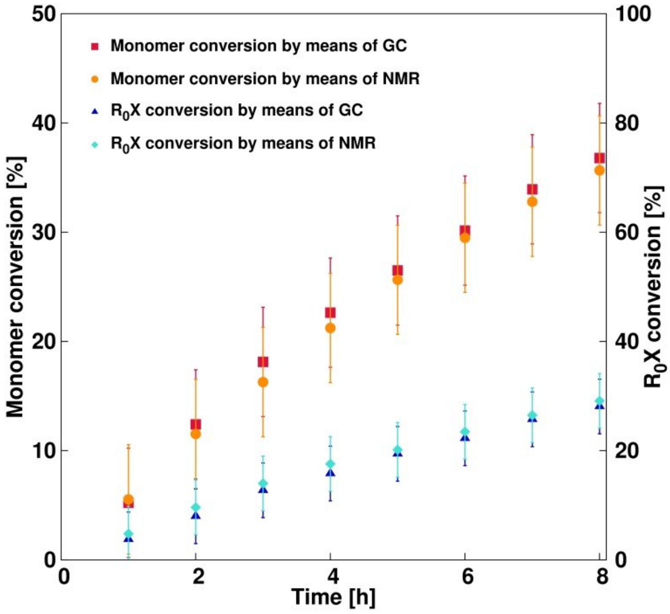

Figure S2: Comparison of monomer and R_0X conversion data via GC (▪, red = X_m; ▲, dark blue = X_{R0X}) and NMR (•, orange = X_m; ◆, light blue = X_{R0X}) for MADIX of styrene at 70°C, selecting OEXEP as initial RAFT agent and AIBN as conventional initiator: Entry 7 in Table S1.

S7. Calculation of the molar amount of end-groups in a polystyrene sample, necessary for the calculation of Equation 8 of the main text.

The three molar amounts in Equation (8) of the main text can be calculated from the elemental analysis results:

$$n(I)=\frac{w(N)\,m_s}{M(N)} \tag{S7}$$

$$n(X) = \frac{w(S)\, m_s}{2\, M(S)} \qquad \text{(S8)}$$

$$n(R_0) = n(X) \qquad \text{(S9)}$$

with *w(A)* (*A*=*N* and *S*) the mass fraction of nitrogen and sulphur, m_s the mass of the elemental analysis sample, and *M(A)* (*A* = *N* and *S*) the molar mass of nitrogen and sulphur. Equation (S9) assumes a negligible contribution of termination between individual R_0 species (R_0R_0 formation) and chain transfer of R_0 to monomer, which is valid in the present work as shown in Section S8 of the Supporting Information

S8. Verification of the negligible contribution of termination between R_0 species and chain transfer of R_0 to monomer

The EGF values mentioned in the main text are determined by means of elemental analysis, more precisely by investigating the nitrogen and sulphur peak in the CHNS chromatogram. These two peaks allow to determine the amounts of the *I* and *X* end-groups respectively. However, the elemental analysis chromatogram does not allow the direct calculation of the amount of R_0 end-groups. Nonetheless, this can be easily overcome by assuming that the number of R_0 end-groups is equal to the number of *X* end-groups, as a new *X* end-group can only be produced by the simultaneous generation of an R_0 which will in turn initiate a new chain. However, this equality only holds up if each R_0 effectively generates a new chain and hence, does not terminate by recombination with another R_0 radical or by chain transfer to monomer.

Figure S3 depicts the rate of termination and chain transfer to monomer of R_0 radicals over the overall consumption rate of R_0 radicals (Entry 3 in Table S1, similar values for other entries of Table S1, simulation achieved by rate coefficients mentioned in Table S3). As clearly visible, the contribution of these reactions are negligible and consequently the number of R_0-end groups can be considered to be equal to the number of *X*-end groups.

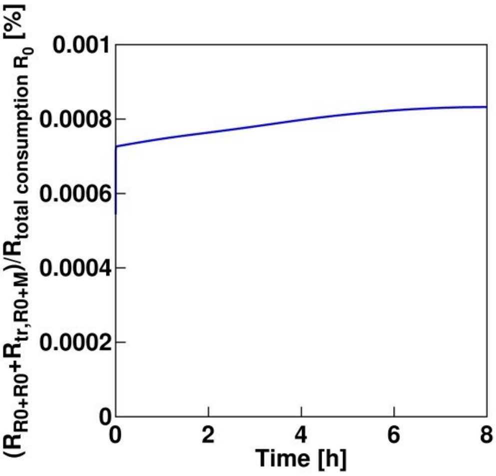

Figure S3: The rate of termination of R_0 radicals by recombination with another R_0 radical or by chain transfer to monomer over the overall consumption rate of R_0 radicals as a function of time (h); Entry 3 in Table S1.

S9. Importance of end-groups obtained by chain transfer to monomer with macroradicals

The EGF values mentioned in the main text are determined by calculating the number of X, R_0 and I end groups. However, when chain transfer to monomer by macroradicals is significant, styryl and H end-groups are possible as well, complicating the EGF calculation. Nonetheless, as shown in Figure S4, under the conditions investigated in this work, these chain transfer reactions do not contribute significantly to the average polymer properties. Consequently, the EGF can be determined by solely investigating the number of X, R_0 and I end- groups.

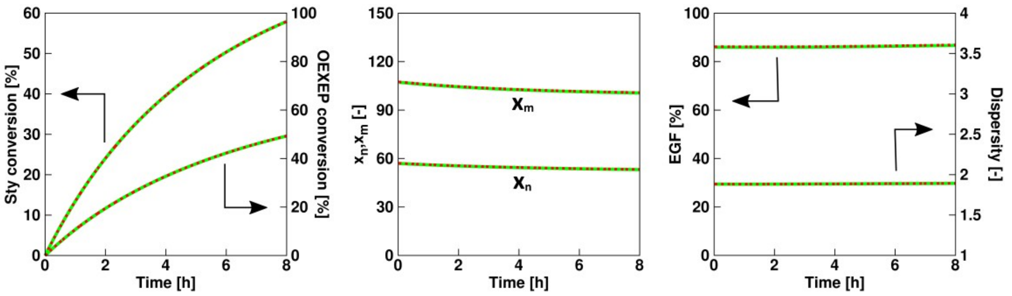

Figure S4: Investigation of the influence of chain transfer to monomer reactions on the monomer and R_0X conversion, number/mass average molar mass, EGF and dispersity: chain transfer to monomer taken into account: solid green line; not taken into account: dotted red line; Entry 3 in Table S1; Rate coefficients as mentioned in Table S3

S10. Evaluation of the need for the use of the correct reaction volume for the kinetic Monte Carlo simulations

The aforementioned extension of the *k*MC procedure enables tracking of the monomer incorporation and possible short chain branch formation for individual macrospecies of a representative polymer sample (e.g. 10^5 polymer chains). For copolymerization processes this implies knowledge of the exact location of the comonomer units along each of the different polymer chains. Specifically for block copolymer synthesis, the contribution of off-spec (homo)polymer chains can be easily detected and the individual block lengths are readily available, as illustrated previously for RDRP techniques based on the so-called persistent radical effect,[2] i.e. atom transfer radical polymerization (ATRP) and nitroxide mediated polymerization (NMP).[3] In the present work, for the first time, the microstructure of individual polymer chains for degenerative RAFT block copolymerization is visualized based on *k*MC simulations, for styrene and *n*BuA as comonomers, OEXEP as initial RAFT agent, and AIBN as conventional radical initiator. It should be stressed that in contrast to traditional ATRP and NMP processes, new (short) chains are continuously formed by I_2 decomposition and further chain growth. This requires a very careful evaluation of the *k*MC reaction volume to be used (>> 10^5 chains) to ensure that the polymer microstructure is accurately represented.

Firstly, the volume needs to be large enough to ensure a good representation of all species present. Small volumes will result in a faulty amount of low concentration species, *e.g.* macroradicals, and consequently in an incorrect simulation of the reactions making use of these species. Secondly, although larger volumes can overcome this issue, it comes at a cost of longer simulation times. Hence, accurate and pragmatic simulation results can only be obtained by considering a proper reaction volume. Practically, this can be achieved by investigating a small reaction volume and increasing it until a convergence of the results is obtained. This guarantees appropriate results within a minimum amount of calculation time. Figure S5 shows the outcome of a kinetic Monte Carlo simulation (Entry 3 in Table S1) for three different reaction volumes. As clearly can be observed, a too small volume (~10^{-17}L; red full line) leads to erroneous results as increasing the volume (~10^{-16}L; dashed green line) results in a different outcome. Increasing the volume even more (~10^{-15}L; dashed blue line) does not result in a change of the outcome but only in a significant longer necessary simulation time (X_m=0.58).

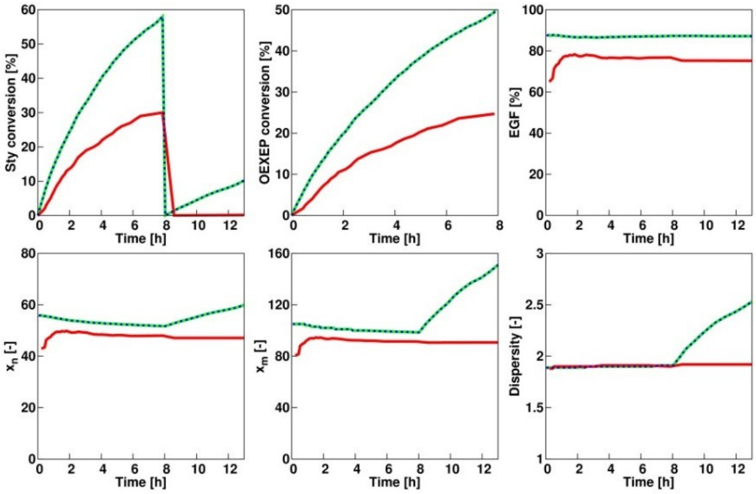

Figure S5: Influence of the reaction volume on the kinetic Monte Carlo simulation; solid red line: V=1.28 x 10^{-17} L; solid green line: V=1.28 x 10^{-16} L; dashed blue line: V=1.28 x 10^{-15} L; 0-8h: entry 3 in the Supporting Information in Table S1; 8-13h: entry 3 in the Supporting Information in Table S2; Reaction coefficients as mentioned in Table S3; clearly the red lines are inaccurate.

S11. Comparison of simulated average characteristics of the extended method of moments and kinetic Monte Carlo (kMC) model

As shown below, the simulated average characteristics of both computational methods converge.

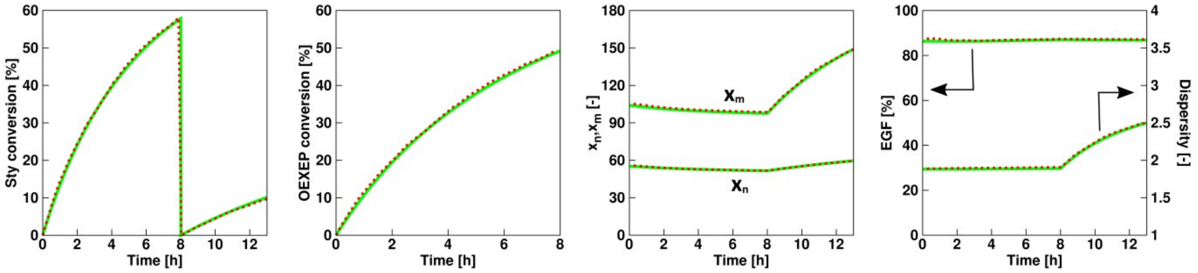

Figure S6: Comparison of monomer and OEXEP (*R_0X*) conversion, number/mass average molar mass (*$x_{n/m}$*), EGF and dispersity (*Đ*) obtained by extended method of moments model (solid green line) and *k*MC model (dotted red line); 0-8h: entry 3 in the Supporting Information in Table S1; 8-13h: entry 3 in the Supporting Information in Table S2.

S12. Demonstration of kinetic insignificance of transfer coefficient $k_{-tr,0}$

The transfer coefficient $k_{-tr,0}$ is defined as the rate coefficient of the reaction of a RAFT leaving group radical R_0 and a dormant macroradical R_iX, resulting in the initial RAFT agent R_0X and a macroradical R_i:

$$R_0^\bullet + R_iX \xrightarrow{k_{-tr,0}} R_0X + R_i^\bullet$$

Figure S7 shows the average polymer properties as a function of time, and the fraction of the R_0 radicals consumed by the reaction shown above as a function of monomer conversion obtained by simulations with k_{-}

$_{tr,0}$=0 L mol^{-1} s^{-1} (green) and $k_{-tr,0}$=100* $k_{tr,0}$ (red, other parameters as in Table S3, Entry 3 in Table S1). As no difference in the prediction of the average polymer properties can be observed, $k_{-tr,0}$ can be considered to be kinetically insignificant and a value of 0 L mol^{-1}s^{-1} can be used for the simulations, simplifying both the model and the parameter estimation of other transfer coefficients ($k_{tr,0}$ and k_{tr}). R_0 will dominantly react with monomer, initiating new growing macroradicals, or with other (macro)radicals, forming new dead (macro)species.

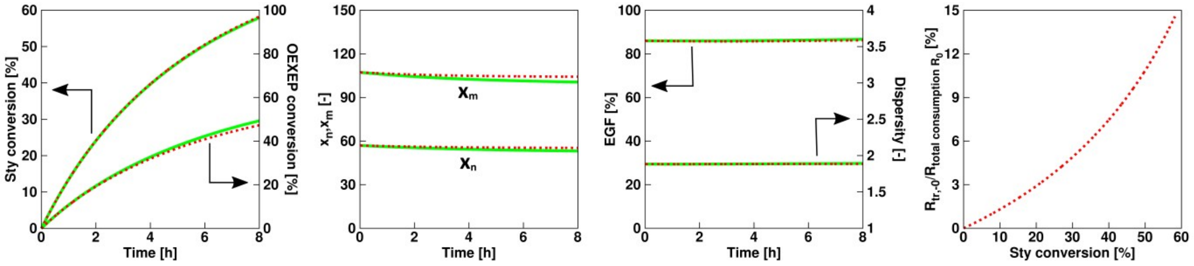

Figure S7: The average polymer properties as a function of time and the fraction of the R_0 radicals consumed by the reaction shown above as a function of monomer conversion obtained by simulations with $k_{-tr,0}$=0 L mol^{-1} s^{-1} (green) and $k_{-tr,0}$=100* $k_{tr,0}$ (red, other parameters as in Table S3, Entry 3 in Table S1)

S13. Demonstration of kinetic insignificance of transfer between initiator radicals (I) and initial RAFT agent (R_0X)

In addition to the exchange reaction between macroradicals (R_i) and the initial RAFT agent (R_0X), exchange between initiator radicals (I) and R_0X can occur as well. This leads to a new dormant IX species which can in turn react with R_i or R_0:

$$I + R_0X \overset{k_{tr,IR0X}}{\rightarrow} IX + R_0$$

$$R_i + IX \overset{k_{tr,RiIX}}{\rightarrow} R_iX + I$$

$$R_0 + IX \overset{k_{tr,R0IX}}{\rightarrow} R_0X + I$$

Assuming for simplicity $k_{tr,RiIX}$ = $k_{tr,0}$ and $k_{tr,R0IX}$ = 10$k_{tr,0}$ (based on k_{pR0} = 10k_p as shown in Table S3), the average polymer properties as a function of time by simulations with $k_{tr,IR0X}$ = 0 L mol^{-1} s^{-1} or $k_{tr,IR0X}$ = 100$k_{tr,0}$ show no significant differences as shown in Figure S8. Consequently, the reaction between I and R_0X can be neglected and I will dominantly initiate new chains by reaction with monomer.

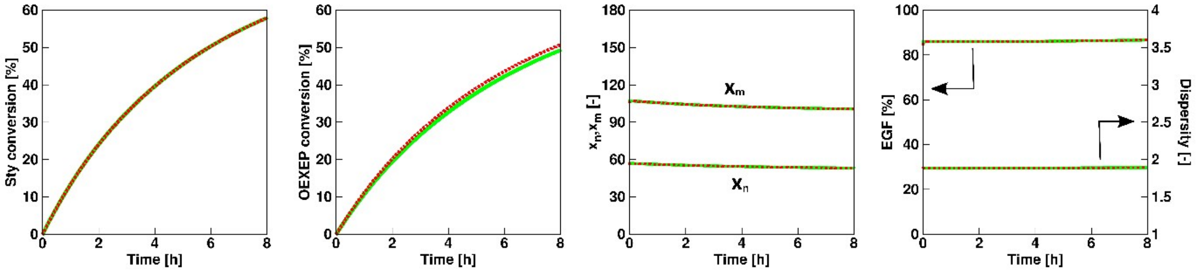

Figure S8: The average polymer properties as a function of time obtained by simulations with $k_{tr,IR0X}$ = 0 L mol^{-1} s^{-1} (green) and $k_{tr,IR0X}$ = 100$k_{tr,0}$ (red, other parameters as in Table S3, Entry 3 in Table S1)

S14. Overview of the reactions and kinetic parameters for the homopolymerization and chain extension with styrene.

An overview of the reactions considered and the corresponding rate coefficients can be found in Table S3.

Table S3: Overview of the reactions and rate coefficients (monomer: styrene) with I_2, $I^\bullet$, M, $R_0^\bullet$, $R_i^\bullet$, P_i, R_0X, R_iX: conventional radical initiator, initiator fragment, monomer, RAFT leaving group, macroradical (chain length i≥1), dead polymer species, initial RAFT agent, dormant macrospecies; 70°C; for termination apparent rate coefficients with given value the one of $k_{t,app}^{1,1}$ (see also further).

Reaction	Equation	k (L mol^{-1} s^{-1})	ref
Dissociation$^{(a)}$	$I_2 \overset{f,k_{dis}}{\rightarrow} 2I^\bullet$	$4.4\ 10^{-5}$	4
Chain Initiation	$I^\bullet + M \overset{k_{pI}}{\rightarrow} R_1^\bullet$	$5.2\ 10^{3}$	5
	$R_0^\bullet + M \overset{k_{pR_0}}{\rightarrow} R_1^\bullet$	$5.1\ 10^{3}$	(b)
Propagation	$R_i^\bullet + M \overset{k_p}{\rightarrow} R_{i+1}^\bullet$	$4.8\ 10^{2}$	6
Chain transfer to monomer	$R_0^\bullet + M \overset{k_{trM,0}}{\rightarrow} R_1^\bullet + P_0$	$2.0\ 10^{-2}$	(c)
	$R_i^\bullet + M \overset{k_{trM}}{\rightarrow} R_1^\bullet + P_i$	$2.0\ 10^{-2}$	7
Termination by recombination	$R_0^\bullet + R_0^\bullet \overset{k_{tc,00}}{\rightarrow} P_0$	$2\ 10^{8.7}$	8,9
	$R_0^\bullet + R_i^\bullet \overset{k_{tc,0}}{\rightarrow} P_i$	$2\ 10^{8.7}$	8,9
	$R_i^\bullet + R_j^\bullet \overset{k_{tc,app}^{i,j}}{\rightarrow} P_{i+j}$	$2\ 10^{8.7}$	8,9
RAFT exchange$^{(f)}$	$R_i^\bullet + R_0X \overset{k_{tr,0}}{\rightarrow} R_iX + R_0^\bullet$	$(3.8\ \pm 0.1)\ 10^{2}$	(d)
	$R_i^\bullet + R_jX \overset{k_{tr}}{\rightarrow} R_iX + R_j^\bullet$	$(2.1 \pm 0.4)\ 10^{2}$	(e)

(a) (apparent) efficiency *f:* see Subsection c; (b) see Subsection b; (c) rate coefficient assumed identical as the rate coefficient for the macroradical; (d) obtained by regression analysis to an extensive set of experimental data (Figure S10, Figure 5 and 6): *F*-value=1.08 10^4; tabulated *F*-value: 4.84; $k_{tr\text{-}0}$ kinetically insignificant (see Subsection S12); (e) obtained by regression analysis to an extensive set of experimental data (Figure 10): *F*-value=1.71 10^3; tabulated *F*-value: 4.84; corresponding $C_{tr,0}$: 0.80±0.02 and C_{tr}: 0.44±0.07; (f) first exchange only important if still R_0X (see Figure S11) present (reverse exchange can be always neglected), second one only relevant upon R_0X removal followed by chain extension (see main text).

The (apparent) termination rate coefficient, the intrinsic rate coefficient concerning chain initiation by the RAFT leaving group R_0, and the (apparent) conventional initiator efficiency are discussed more in depth below.

a. *Apparent termination rate coefficient*

In order to accurately describe the diffusion-controlled mechanism of bimolecular termination in radical polymerization, the composite k_t model[8] (aka RAFT-CLD-T model) was used. This model allows to calculate an apparent homotermination rate coefficient ($k_{tc,app}^{i,i}$; *i*=chain length; only considering termination by recombination) dependent on the chain length *i* and the polymer mass fraction m_p (and thus monomer conversion X_m):

For $i < i_{gel}$

$$k_{tc,app}^{i,i} = k_t^{1,1}\, i^{-\alpha_S} \qquad \text{for } i < i_{SL} \tag{S10}$$

$$k_{tc,app}^{i,i} = k_t^{1,1}\, i_{SL}^{(\alpha_L - \alpha_S)}\, i^{-\alpha_S} \qquad \text{for } i \geq i_{SL} \tag{S11}$$

For $i \geq i_{gel}$

$$k_{tc,app}^{i,i} = k_t^{1,1}\, i_{SL}^{(\alpha_{gel} - \alpha_S)}\, i^{-\alpha_{gel}} \qquad \text{for } i < i_{SL} \tag{S12}$$

$$k_{tc,app}^{i,i} = k_t^{1,1}\, i_{SL}^{(\alpha_L - \alpha_S)}\, i^{(\alpha_{gel} - \alpha_L)}\, i^{-\alpha_{gel}} \qquad \text{for } i \geq i_{SL} \tag{S13}$$

with $k_t^{1,1}$ the (apparent) termination rate coefficient for radicals with chain length 1, α_S the exponent for termination for termination of short chains in dilute solution, α_L the exponent for long chains in dilute solution, α_{gel} the exponent for chains in the gel regime, i_{SL} the crossover chain length between short- and long-chain behavior, i_{gel} the chain length at the onset of the gel-effect. An overview of these parameters can be found in Table S4.[8–10]

From the apparent homotermination rate coefficients, the apparent cross-termination rate coefficient $k_{tc,app}^{i,j}$ is calculated for simplicity using the geometric mean:

$$k_{tc,app}^{i,j} = \sqrt{k_{tc,app}^{i,i}\, k_{tc,app}^{j,j}} \tag{S14}$$

An averaged (zero order) apparent termination rate coefficient can be calculated at any moment :

$$\langle k_{tc,app} \rangle = \frac{\sum_{i=1}^{\infty}\sum_{j=1}^{\infty}(1+\delta_{ij})k_{tc,app}^{i,j}[R_i][R_j]}{\left(\sum_{i=1}^{\infty}[R_i]\right)^2} \tag{S15}$$

with δ_{ij} the Kronecker Delta Function. When employing the kinetic Monte Carlo technique, each macroradical R_i is tracked individually and Equation (S15) can be calculated exactly. However, when applying the deterministic extended method of moments method this information is not available. Nonetheless, Equation (S15) can still be approximately used by considering the Flory-Schulz distribution to obtain the macroradical chain length distribution:[11]

$$f_n(i) = \frac{1}{x_{n,r}}exp\left(-\frac{i}{x_{n,r}}\right) \tag{S16}$$

with $f_n(i)$ the number fraction of macroradicals with chain length i and $x_{n,r}$ the associated number average chain length.

For the validation of the Flory-Schulz distribution for the macroradical CLD in the present work, the reader is referred to the main text.

Table S4: Parameters used for the composite k_t model; monomers: styrene (Sty) and methyl acrylate (MA; related to next subsection: these parameters were used for *n*-butyl acrylate simulations as a first approximation); m_p: polymer mass fraction

Monomer	**T(K)**	$k_t^{1,1}$	α_S	i_{SL}	α_L	α_{gel}	i_{gel}
Sty	363	$2\times10^{8.7}$	0.53	30	0.15	$1.22m_p$-0.11	$3.30m_p^{-2.13}$
MA	323	See Table S6	0.78	18	0.15	$0.81m_p$-0.05	$6.9m_p^{-2.2}$

b. Chain initiation by RAFT leaving group (R_0)

The RAFT leaving group R_0 is identical to an ethyl acrylate radical. As a result, the rate coefficient of the reinitiation reaction (k_{pR_0}) can be assessed by considering the propagation rate coefficient of poly(ethyl acrylate) radicals to styrene, ignoring possible chain length dependencies. This rate coefficient can be assessed using the rate coefficient of the homopolymerization of ethyl acrylate and the monomer reactivity ratio r_{EA}:

$$r_{EA} = \frac{k_{p,EAEA}}{k_{p,EASty}} \tag{S17}$$

$$k_{pR_0} \approx k_{p,EASty} = \frac{k_{p,EAEA}}{r_{EA}} \tag{S18}$$

Using a reactivity ratio r_{EA} of 0.22 as determined by Brar et al. [12] and a homopropagation rate coefficient $k_{p,EAEA}$ of 1117 L mol^{-1} s^{-1} at 70°C as mentioned by Gao et al. [13], a k_{pR_0}= 5077 L mol^{-1} s^{-1} results. Note that this value is as good as identical as the one for the other chain initiation.

c. *Apparent conventional initiator efficiency*

An apparent conventional initiator efficiency f_{app} dependent on monomer conversion X_m can be calculated as described by Buback *et.al.*:[14]

$$f_{app} = \frac{D_I}{D_I + D_{term}} \tag{S19}$$

with D_I the diffusion coefficient of the cyanoisopropyl radical and $D_{term} = 5.3\ 10^{-10} m^2 s^{-1}$ a correction factor related to the rate of termination between two cyanoisopropyl radicals.

Table S5: Parameters used to calculate the apparent initiator efficiency (Equation (S17 - (S19) as described by Buback *et al.*[14] for AIBN as conventional radical initiator and styrene as monomer.

Parameter	Description	Value
$D_{0,I}\ (m^2 s^{-1})$	Pre-exponential factor for diffusion	$1.95\ 10^{-4}$
$E_I\ (kJ\ mol^{-1})$	Activation energy for diffusion	31
$R\ (J\ mol^{-1} K^{-1})$	Universal gas constant	8.314
$T\ (K)$	Temperature	$333 - 363$
$w_1\ (-)$	Mass fraction of monomer	0-1
$w_2\ (-)$	Mass fraction of polymer	0-1
$V_1^*\ (m^3 mol^{-1})$	Specific critical hole free volume of monomer [(a)]	$9.46\ 10^{-7}$
$V_2^*\ (m^3 mol^{-1})$	Specific critical hole free volume of polystyrene	$8{,}50\ 10^{-7}$
$\frac{K_{11}}{\lambda}\ (m^3\ kg^{-1}\ K^{-1})$	Parameter for specific hole free volume monomer [(a)]	$1.49\ 10^{-9}$
$\frac{K_{12}}{\lambda}\ (m^3\ kg^{-1}\ K^{-1})$	Parameter for specific hole free volume polymer	$5.82\ 10^{-10}$
$K_{21} - T_{g1}\ (K)$	Parameter for specific hole free volume monomer [(a)]	-84
$K_{22} - T_{g1}\ (K)$	Parameter for specific hole free volume polymer	-327
$\xi_{i2}\ (-)$	Critical jumping unit volume ratio for cyanoispropyl radical to polymer	0.36
$\xi_{12}\ (-)$	Critical jumping unit volume ratio for monomer to polymer	0.59

(a) Ethylbenzene used as model compound.

According to the free volume theory, D_I can be calculated via:

$$D_I = D_{0,I}\exp\left(-\frac{E_I}{RT}\right)\exp\left(\frac{-w_1 V_1^* \xi_{i2}/\xi_{12} + w_2 V_2^* \xi_{12}}{V_{FH}/\lambda}\right) \tag{S20}$$

$$\frac{V_{FH}}{\lambda} = \frac{K_{11}}{\lambda} w_1\left(K_{21} - T - T_{g1}\right) + \frac{k_{12}}{\lambda} w_2\left(K_{22} + T - T_{g1}\right) \tag{S21}$$

Table S5 gives an overview of the description and value of the parameters used in Equation (S18) and (S19).

S15. Reactions and kinetic parameters for chain extension with n-butyl acrylate

The reactions and rate coefficients to investigate the chain extension of dormant polystyrene with n-butyl acrylate are mentioned in Table S6, neglecting chain transfer to monomer, backbiting and β-scission. The actual apparent termination reactivity is calculated by averaging the RAFT-CLD-T value for pure polystyrene and pure poly(n-butyl acrylate), according to the number of monomer units of each type being incorporated on an overall basis.

Table S6: Overview of the reactions and rate coefficients (extension of polystyrene with monomer *n*-butyl acrylate (*n*BuA)) with $I^\bullet$, M, $R_i^\bullet$, P_i, R_iX: initiator fragment, monomer (*n*BuA), macroradical (chain length i≥1), dead polymer species, dormant macrospecies; $R_{nB,i}^\bullet$ and $R_{S,i}^\bullet$: macroradical with chain length *i* and *n*-butyl acrylate (nB) and styrene (S) as terminal unit; 60°C; for termination apparent rate coefficients averaging with respect to composition.

Reaction	Equation	k (L mol^{-1} s^{-1})	Ref
Dissociation	$I_2 \xrightarrow{f,k_{dis}} 2I^\bullet$	$1.1\ 10^{-5}$	4
Chain Initiation	$I^\bullet + M \xrightarrow{k_{pI}} R_{nB,1}^\bullet$	$4.0\ 10^{3}$	(a)
Propagation	$R_{nB,i}^\bullet + M \xrightarrow{k_{pnBnB}} R_{nB,i+1}^\bullet$	$3.4\ 10^{4}$	15
	$R_{S,i}^\bullet + M \xrightarrow{k_{pSnB}} R_{nB,i+1}^\bullet$	$4.8\ 10^{2}$	(b)
Termination by recombination	$R_{nB,i}^\bullet + R_{nB,j}^\bullet \xrightarrow{k_{tc,app}^{i,j}} P_{i+j}$	$1.3\ 10^{9}$	16,(c)
Termination by disproportionation	$R_{nB,i}^\bullet + R_{nB,j}^\bullet \xrightarrow{k_{td,app}^{i,j}} P_i + P_j$	$1.3\ 10^{9}$	16,(c)
RAFT exchange$^{(e)}$	$R_{nB,i}^\bullet + R_{S,j}X \xrightarrow{k_{tr,nBS}} R_{nB,i}X + R_{S,j}^\bullet$	4.6×10^{4}	(d)

(a) taken identical as reaction with styrene for simplicity; (b) calculated by means of the monomer reactivity ratio[17,18] $r = {}^{k_{p,SS}}/_{k_{p,SnBa}} = 0.71$; (c) with ${}^{k_{tc}}/_{k_{td}} = 0.9$; (d) obtained by fitting to experimental data (Figure 14); corresponding C_{tr}: 1.35; (e) other exchanges can be neglected as kinetically insignificant (see Figure S16). Styrene radicals first add to *n*BuA based on preliminary screening.

S16. Inefficient removal of unreacted R$_0$X (OEXEP) via precipitation

In order to determine the end-group functionality (EGF) of the synthesized MADIX polystyrene polymers and to efficiently investigate the chain extension of these polymers, unreacted R$_0$X (OEXEP) needs to be removed. Due to the high dispersity associated with the bulk polymerization of styrene in the presence of a xanthate-type RAFT agent, conventional methods such as precipitation are not recommended as this would result, next to the removal of R_0X, in the significant loss of the low molar mass polymer chains as shown in Figure S3 (dashed blue line vs solid red line). Consecutive precipitation was here performed by dissolving the polymer samples in a minimum amount of toluene and slowly adding it to cold methanol. A much more suited experimental procedure is dialysis (coinciding dashed blue and dotted green line in Figure S9) as this does not alter the SEC trace. For more information on the dialysis procedure and the confirmation of the complete removal of non-macromolecules such as styrene and OEXEP, the reader is referred to the main text.

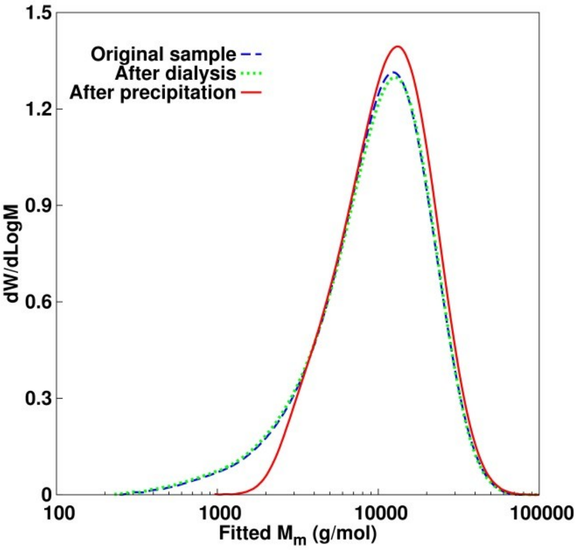

Figure S9: SEC data illustrating the loss of low-molar mass polymer chains if precipitation is used. Dialysis results in the preservation of all chains; dashed blue line: original polymer sample, dotted green line: polymer sample after dialysis, solid red line: polymer sample after precipitation in cold methanol; Entry 1 in Table S1, X_m=0.33

S17. The effect of TCL on the homopolymerization of styrene in the presence of (O-ethyl xanthate)-2- ethyl propionate and a fixed $[R_0X]_0/[I_2]_0$

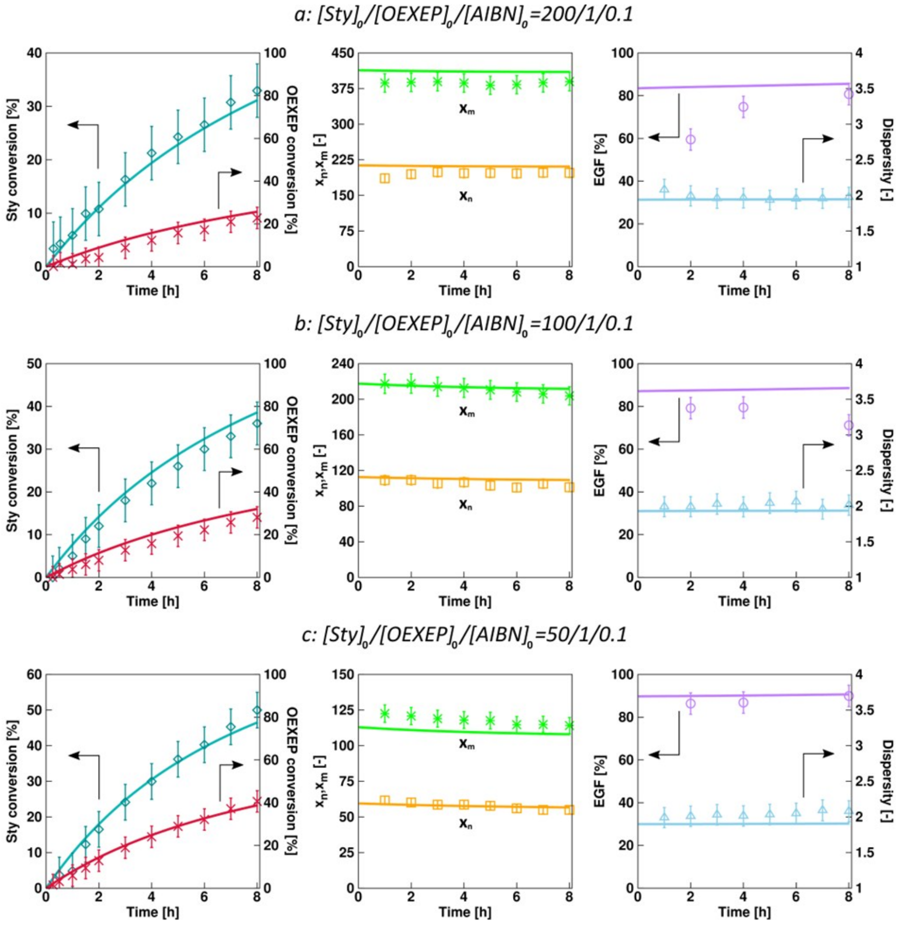

a: $[Sty]_0/[OEXEP]_0/[AIBN]_0=200/1/0.1$

b: $[Sty]_0/[OEXEP]_0/[AIBN]_0=100/1/0.1$

c: $[Sty]_0/[OEXEP]_0/[AIBN]_0=50/1/0.1$

Figure S10: Comparison between simulations and experiments (next to Figure 5 and 6 in the main text; entry 2, 6 and 7 in Table S1).

S18. Demonstration of kinetic insignificance of transfer coefficient k_{tr} during homopolymerization experiments

The transfer coefficients $k_{tr,0}$ and k_{tr} are defined as the rate coefficient of the reaction of a macroradical and respectively a RAFT agent R_0X and a dormant macrospecies R_iX. Figure S11 shows the average polymer properties as a function of time obtained by simulations with k_{tr}=0 L mol^{-1} s^{-1} (green) and $k_{tr}=10k_{tr,0}$ (red, other parameters as in Table S3) during a homopolymerization experiment (Entry 3 in Table S1). As no difference in the prediction of the average polymer properties can be observed, k_{tr} can be considered to be kinetically insignificant and a value of 0 L mol^{-1}s^{-1} can be used for the simulations, simplifying the estimation of $k_{tr,0}$.

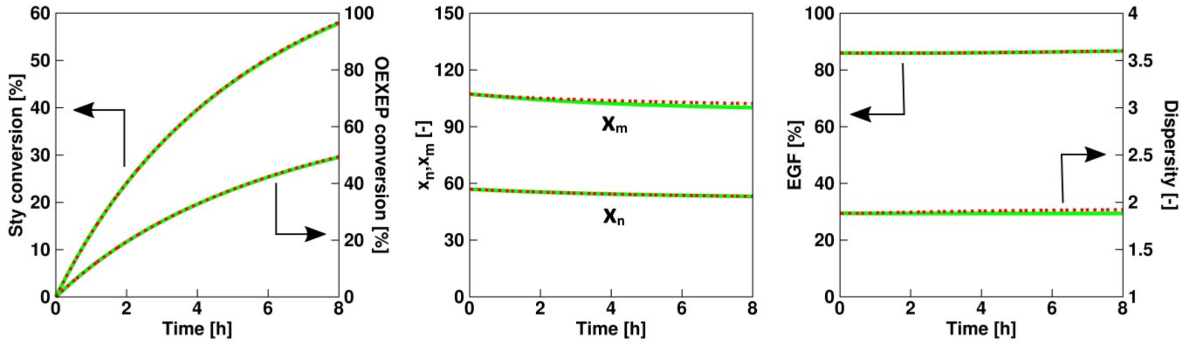

Figure S11: The average polymer properties as a function of time obtained by simulations with k_{tr}=0 L mol^{-1} s^{-1} (green) and $k_{tr}=10k_{tr,0}$ (red, other parameters as in Table S3, Entry 3 in Table S1)

S19. Determination of $C_{tr,0}$ via the methods of Moad and Mayo

The methods of Moad and Mayo are often applied to determine the $C_{tr,0}$ value in MADIX when low values (<10) are expected by examining the slope of ln([R_0X]) vs ln([M]) (Moad) or $1/x_n$ vs [R_0X]$_0$/[M]$_0$ (Mayo).[19–24] Figure S12 and Table S7 give an overview of the results after application of both methods on the experimental data discussed in this work (Table S1).

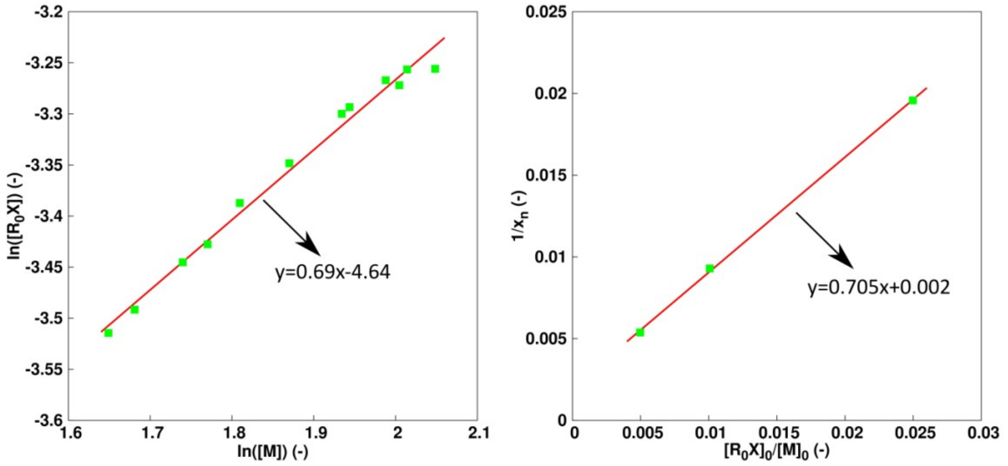

Figure S12: Example of the use of the method of Moad (left; Entry 6 in Table S1) and the method of Mayo (right; Entry 4,5 and 6 in Table S1; identical [I_2]$_0$) for the determination of $C_{tr,0}$

The method of Moad results in a $C_{tr,0}$ of 0.69±0.04 (Table S7; one example in Figure S12: left). The method of Mayo leads to a value of 0.71±0.02 (Figure S12 right).

Table S7: Application of the method of Moad on the experiments shown in Table S1 for the determination of $C_{tr,0}$

Entry in Table S1	$C_{tr,0}$
1	0.66
2	0.75
3	0.73
4	0.63
5	0.68

6	0.69
7	0.73
Average	**0.69±0.04**

S20. Limitations of the method of Mayo for determining $C_{tr,0}$

The method of Mayo was originally developed to determine the transfer coefficient (C_{tr}) for chain transfer with solvent in the radical polymerization of styrene.[22] Later, this method has been often used in literature[20,24–26] to determine C_{tr} of other reactants. Strictly the kinetic chain length (ν), which is related to the number average chain length of the actual polymer (no radicals) that is experimentally accessible, is needed. For the RAFT CTA in the present work this ν is given by:

$$\nu = \frac{k_p[M][R_{tot}]}{k_{trM}[M][R_{tot}] + k_{tr,0}[R_0X][R_{tot}] + k_{tc}[R_{tot}][R_{tot}]} \tag{S22}$$

with $k_{p,/rM/tr0/tc}$ the rate coefficient for propagation, chain transfer to monomer, transfer to R_0X and termination by recombination (no correction factor as strict definition on radical level and total concentration), considering only termination by recombination as termination event and assuming that the obtained polymer has undergone only a single transfer event (k_{tr}=0, as justified by Supporting Information Section S18).

Taking the reciprocal and introducing $C_{tr,0} = k_{tr,0}/k_p$ and $C_M = k_{trM}/k_p$, Equation (S22) is transformed in:

$$\frac{1}{\nu} = C_M + \frac{k_{tc}[R_{tot}]}{k_p[M]} + C_{tr,0}\frac{[R_0X]}{[M]} \tag{S23}$$

which is known as the Mayo equation and is often written as:

$$\frac{1}{\nu} = C_M + \frac{1}{\nu_0} + C_{tr,0}\frac{[R_0X]}{[M]} \tag{S24}$$

with ν_0 the kinetic chain length in absence of chain transfer.

At low monomer conversion, $[R_0X]/[M]$ can be considered constant and equal to the initial ratio $[R_0X]_0/[M]_0$. Consequently, by performing several experiments with varying $[R_0X]_0/[M]_0$, $C_{tr,0}$ can be determined by the slope of ν^{-1} vs $[R_0X]_0/[M]_0$ plot if ν_0^{-1} is independent of that ratio. As discussed thoroughly by Smulders[27], this can be expected if the same initiator amount is used for all the experiments, the re-initiation rate of the RAFT leaving group radical (R_0) is high, sufficiently fast fragmentation takes place, and k_{tc} and $[R_i]$ are independent of $[R_0X]_0/[M]_0$.

However, more important and often ignored, *ν* represents the average number of monomer units of the macroradicals *before* their termination by recombination or chain transfer, and is not necessarily equal to the related experimentally determinable number average chain length x_n. For example, in absence of chain transfer and with thus only termination by recombination as termination event, x_n is equal to twice the kinetic chain length, not taking into account end-groups, whereas when chain transfer is the dominant chain stopping event and the EGF approaches 1, x_n will be equal to v.

In order to assess the validity of the Mayo equation in this work, the approximation of the number average chain length of the radicals by the overall chain length needs to be verified. As shown in Figure S13 (left), for a reference experiment (Entry 5 in Table S1), this is not the case due to the EGF being significantly lower than 1 and consequently shifting the overall x_n to somewhat higher values. Nonetheless, x_n of the dormant chains (R_iX) and the dead chains (P_i) are approximately equal to, respectively, once and twice the x_n of the macroradicals. Importantly, the small difference between the x_n of the macroradicals or dormant species and the overall x_n does result in a lower value of $C_{tr,0}$ (0.75 vs 0.80; with 0.80 also the value with method presented in present work) as shown in Figure S13 (right). This slight mismatch leads to an incorrect simulation of the MADIX average chain length characteristics in an complete kinetic model (see main text). In conclusion, the Mayo method can only be used to obtain an assessment of $C_{tr,0}$ for the conditions investigated in this work.

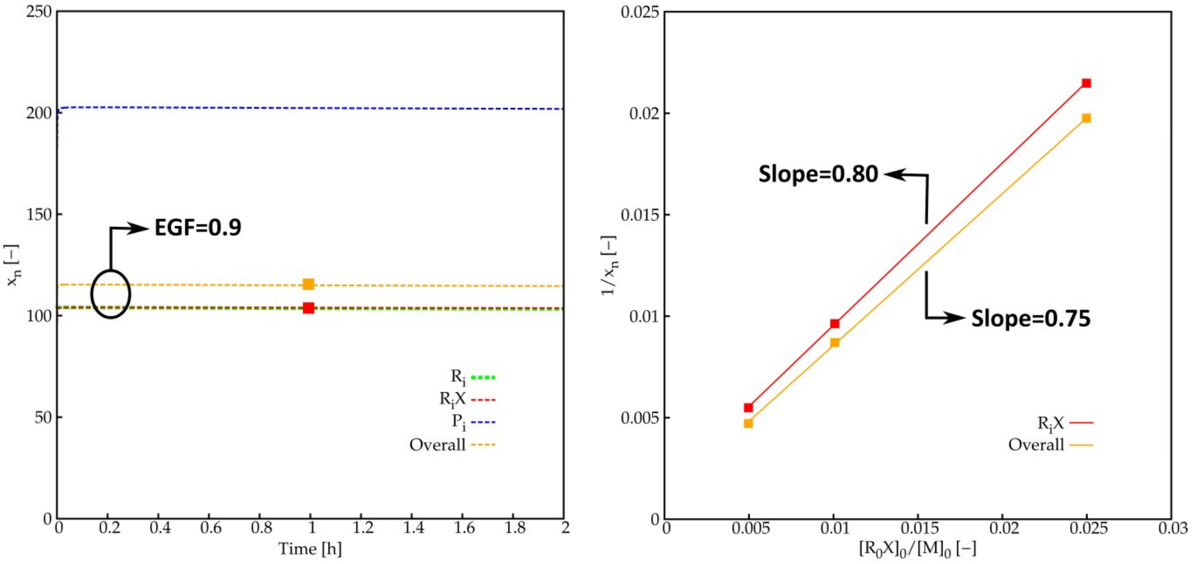

Figure S13: left: number average chain length (x_n) of radicals (green), dormant chains (red), dead chains (blue) and overall (orange) as a function of time for Entry 5 in Table S1; right: Application of the method of Mayo on model output of Entry 4, 5 and 6 in Table S1 (identical $[I_2]_0$) by means of $x_n(R_iX)$ (red squares) and x_n*(overall)* (orange squares, as typically done in practice); lines represent trend lines through the data points; Parameters as mentioned in Table S3; theoretical $C_{tr,0}$ from model=$k_{tr,0}/k_p$=384/479=0.80; $c_{tr,0}$ by means of $x_n(R_iX)$ =0.80 and x_n*(overall)*=0.75

S21. Influence of $[R_0X]_0/[I2]_0$ and $[M]_0/[R0X]_0$ on the R_0X conversion

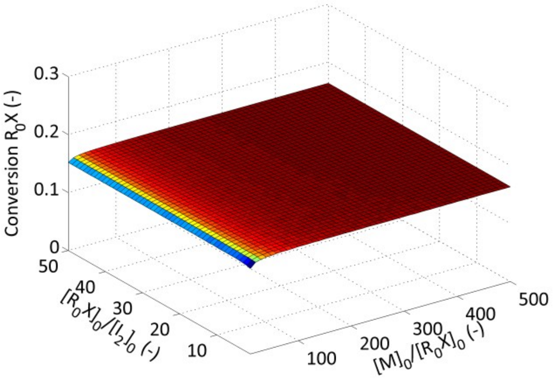

Figure S14: *R_0X* conversion (X_{R_0X}) as a function of [*R_0X*]$_0$/[*I_2*]$_0$ (ranging from 1 to 50) and [*M*]$_0$/[*R_0X*]$_0$ (ranging from 10 to 500); simulated data have been achieved by means of the parameters given in Table S3 with *R_0X*=(O-ethyl xanthate)-2-ethyl propionate, *M*=Sty, and *I_2*=AIBN; 70°C; X_m=20%.

S22. Demonstration of the importance of accurate determination of k_{tr} of exchange between polystyrene macroradicals and dormant polystyrene

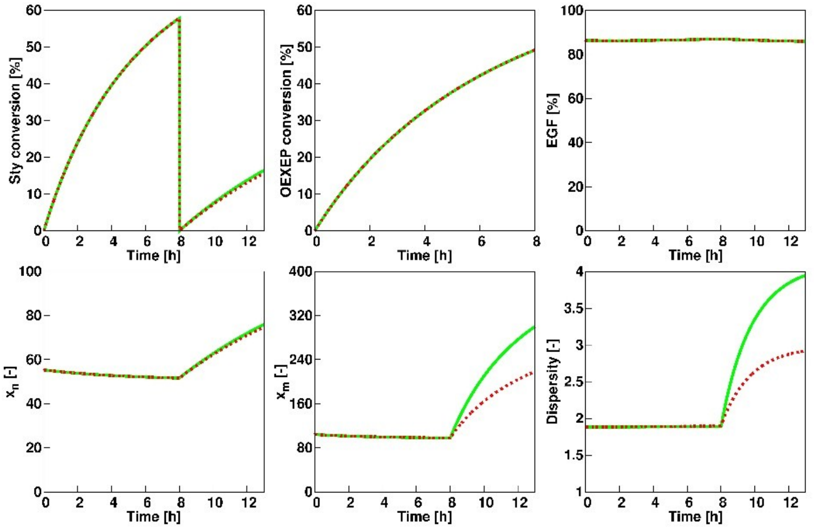

Figure S15: The average polymer properties as a function of time for simulations of the chain extension of dormant polystyrene with fresh styrene (entry 1 in Table S2) with k_{tr}= 2.1 x 10² L mol^{-1} s^{-1} (green, see Table S3) as obtained by regression analysis and k_{tr}=k_{tr},0=3.8 x 10² L mol^{-1} s^{-1} (red, see Table S3). Other parameters as in Table S3

S23. Determination of the kinetically significant transfer coefficients during chain extension of dormant polystyrene with n-butyl acrylate in solution

When considering the chain extension of dormant polystyrene with n-butyl acrylate, four possible RAFT exchange reactions exist as two macroradical and dormant species types are feasible:

$$R_{nBuA,i}^{\bullet} + R_{Sty,j}X \xrightarrow{k_{tr,nBuASty}} R_{nBuA,i}X + R_{Sty,j}^{\bullet}$$

$$R_{nBuA,i}^{\bullet} + R_{nBuA,j}X \xrightarrow{k_{tr,nBuAnBuA}} R_{nBuA,i}X + R_{nBuA,j}^{\bullet}$$

$$R_{Sty,i}^{\bullet} + R_{Sty,j}X \xrightarrow{k_{tr,StySty}} R_{Sty,i}X + R_{Sty,j}^{\bullet}$$

$$R_{Sty,i}^{\bullet} + R_{nBuA,j}X \xrightarrow{k_{tr,StynBuA}} R_{Sty,i}X + R_{nBuA,j}^{\bullet}$$

with $R_{nBuA,i}^{\bullet}$ and $R_{Sty,i}^{\bullet}$ a macroradical with chain length i and n-butyl acrylate (*n*BuA) and styrene (Sty) as terminal unit, and $R_{nBuA,j}X$ and $R_{Sty,j}X$ a dormant macrospecies with chain length i and n-butyl acrylate (*n*BuA) and styrene (Sty) as terminal unit next to the xanthate functional group *X*.

However, as shown in Figure S16, only $k_{tr,n\text{BuASty}}$ will influence the average polymer properties and the other transfer coefficients can be considered kinetically insignificant, reducing the complexity of the model and simplifying the estimation of $k_{tr,n\text{BuASty}}$. Styrene macroradicals, generated by the exchange of dormant polystyrene with *n*BuA macroradicals, will swiftly react with *n*BuA monomer forming again macroradicals with an *n*BuA terminal unit, explaining the insignificance of ktr,StySty and $k_{tr,\text{Sty}n\text{BuA}}$. Futhermore, similarly to the chain extension reaction with fresh styrene (see Figure 10), a single activation-growth-deactivation cycle is performed per chain, resulting in the absence of reactivation of dormant poly(styrene-b-*n*BuA) blockcopolymer and hence the insignificance of $k_{tr,n\text{BuA}n\text{BuA}}$. This can be explained by the low concentration of dormant poly(styrene-b-*n*BuA) compared to the initial dormant polystyrene at low conversions, as shown in Figure S17.

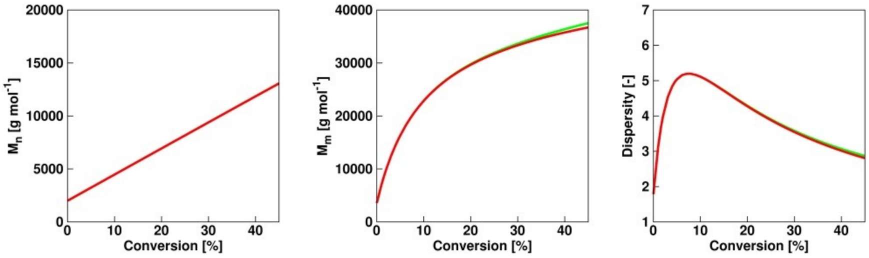

Figure S16: The average polymer chain length properties as a function of time obtained by simulations with (i) $k_{tr,nBuAnBuA}$ = $k_{tr,StySty}$ = $k_{tr,StynBuA}$ = 0 L mol^{-1} s^{-1} and $k_{tr,nBuASty}$ = 4.6 10^{4} L mol^{-1} s^{-1} (full green line), and (ii) for simplicity: $k_{tr,StySty}$ = $k_{tr,StynBuA}$ = 2.1 10^{2} L mol^{-1} s^{-1} and $k_{tr,nBuASty}$ = $k_{tr,nBuAnBuA}$ = 4.6 10^{4} L mol^{-1} s^{-1} (dotted red line); other parameters as in Table S6; simulated output with stochastic method; Conditions: [Toluene]= 6 mol L^{-1}, [n-BuA]=2.0 mol L^{-1}, [n-BuA]/ [R$_{i,sty}$X]/ [AIBN]=198/1/1; T=60°C; Parameters: Table S6

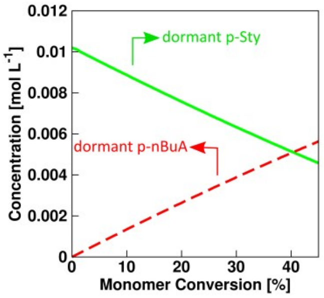

Figure S17: The concentration of dormant polystyrene (green) and dormant poly(styrene-b-nBuA) (red) during the extension of dormant polystyrene with *n*BuA; Conditions: [Toluene]= 6 mol L^{-1}, [n-BuA]=2.0 mol L^{-1}, [n-BuA]/ [$R_{i,sty}$X]/ [AIBN]=198/1/1; T=60°C

References

1 WO 1998058974, 1998.

2 H. Fischer and M. Souaille, *Macromol. Symp.*, 2001, **174**, 231–240.

3 C. Toloza Porras, D. R. D'hooge, P. H. M. Van Steenberge, M. F. Reyniers and G. B. Marin, *Macromol. React. Eng.*, 2013, **7**, 311–326.

4 M. T. Erben and S. Bywater, *J. Am. Chem. Soc.*, 1955, **77**, 3712–3714.

5 K. Heberger and H. Fischer, *Int. J. Chem. Kinet.*, 1993, **25**, 249–263.

6 M. Buback, R. G. Gilbert, R. A. Hutchinson, B. Klumberman, F.-D. Kuchta, B. G. Manders, K. F. O'Driscoll, G. T. Russell and J. Schweer, *Macromol. Chem. Phys.*, 1995, **196**, 3267–3280.

7 A. W. Hui and A. E. Hamielec, *J. Appl. Polym. Sci.*, 1972, **16**, 749–769.

8 G. Johnston-Hall and M. J. Monteiro, *J. Polym. Sci. Part a-Polymer Chem.*, 2008, **46**, 3155–3176.

9 P. Derboven, D. R. D'hooge, M.-F. Reyniers, G. B. Marin and C. Barner-Kowollik, *Macromolecules*, 2015, **48**, 492–501.

10 G. Johnston-Hall and M. J. Monteiro, *Macromolecules*, 2008, **41**, 727–736.

11 E. Mastan, D. Zhou and S. Zhu, *J. Polym. Sci. Part A Polym. Chem.*, 2014, **52**, 639–651.

12 A. S. Brar and Sunita, *Makromol. Chemie*, 1993, **194**, 1707–1720.

13 J. Gao, N. McManus and A. Penlidis, *Macromol. Chem. Phys.*, 1997, **198**, 843–859.

14 M. Buback, B. Huckestein, F. Kuchta and G. T. Russell, *Macromol. Chem. Phys.*, 1994, **195**, 2117–2140.

15 J. M. Asua, S. Beuermann, M. Buback, P. Castignolles, B. Charleux, R. G. Gilbert, R. A. Hutchinson, J. R. Leiza, A. N. Nikitin, J. P. Vairon and A. M. Van Herk, *Macromol. Chem. Phys.*, 2004, **205**, 2151–2160.

16 J. Barth, M. Buback, P. Hesse and T. Sergeeva, *Macromolecules*, 2010, **43**, 4023–4031.

17 X. Li, W. J. Wang, F. Weng, B. G. Li and S. Zhu, *Ind. Eng. Chem. Res.*, 2014, **53**, 7321–7332.

18 L. K. Kostanski and A. E. Hamielec, *Polymer (Guildf).*, 1992, **33**, 3703–3710.

19 M. M. Adamy, A. M. van Herk, M. Destarac and M. J. Monteiro, *Macromolecules*, 2003, **36**, 2293–2301.

20 B. Y. K. Chong, J. Krstina, T. P. T. Le, G. Moad, A. Postma, E. Rizzardo and S. H. Thang, *Macromolecules*, 2003, **36**, 2256–2272.

21 G. Moad, J. Chiefari, Y. K. Chong, J. Krstina, R. T. A. Mayadunne, A. Postma, E. Rizzardo and S. H. Thang, *Polym. Int.*, 2000, **49**, 993–1001.

22 F. R. Mayo, *J. Am. Chem. Soc.*, 1943, **65**, 2324–2329.

23 M. Destarac, C. Brochon, J. M. Catala, A. Wilczewska and S. Z. Zard, *Macromol. Chem. Phys.*, 2002, **203**, 2281–2289.

24 P. Derboven, P. H. M. Van Steenberge, M. Reyniers, C. Barner-kowollik, D. R. D'hooge and G. B. Marin, *Macromol. Theory Simulations*, 2016, **25**, 104–115.

25 J. Chiefari, R. T. A. Mayadunne, C. L. Moad, G. Moad, E. Rizzardo, A. Postma, M. A. Skidmore and S. H. Thang, *Macromolecules*, 2003, **36**, 2273–2283.

26 J. Chiefari, Y. K. B. Chong, F. Ercole, J. Krstina, J. Jeffery, T. P. T. Le, R. T. A. Mayadunne, G. F. Meijs, C. L. Moad, G. Moad, E. Rizzardo, S. H. Thang and C. South, 1998, **31**, 5559–5562.

27 W. W. Smulders, Technische Universiteit Eindhoven, 2002.